Nonlinear dynamics of a rack-pinion-rack device powered by the Casimir force

MirFaez Miri,[1,2,*] Vahid Nekouie,[3] and Ramin Golestanian[4,†]
[1]*Institute for Advanced Studies in Basic Sciences (IASBS), P.O. Box 45195-1159, Zanjan 45195, Iran*
[2]*Department of Physics, University of Tehran, P.O. Box 14395-547, Tehran, Iran*
[3]*Department of Engineering Materials, University of Sheffield, Sheffield S1 3JD, United Kingdom*
[4]*Department of Physics and Astronomy, University of Sheffield, Sheffield S3 7RH, United Kingdom*
(Received 10 September 2009; published 11 January 2010)

Using the lateral Casimir force—a manifestation of the quantum fluctuations of the electromagnetic field between objects with corrugated surfaces—as the main force transduction mechanism, a nanomechanical device with rich dynamical behaviors is proposed. The device is made of two parallel racks that are moving in the same direction and a pinion in the middle that couples with both racks via the noncontact lateral Casimir force. The built-in frustration in the device causes it to be very sensitive and react dramatically to minute changes in the geometrical parameters and initial conditions of the system. The noncontact nature of the proposed device could help with the ubiquitous wear problem in nanoscale mechanical systems.

DOI: 10.1103/PhysRevE.81.016104 PACS number(s): 07.10.Cm, 42.50.Lc, 46.55.+d, 85.85.+j

I. INTRODUCTION

As the ability to fabricate mechanical components with fine geometrical structures improves, engineers face new problems related to wear [1], stiction, and jamming [2–4] of the mechanical devices. Whereas these tribological issues are being tackled using a variety of relatively more conventional methods [5], it will be interesting to investigate the possibility of using physical mechanisms that allow the different parts of mechanical devices to engage without using direct contact between them.

It has been suggested recently that due to its strong distance dependence, the Casimir force [6–8] could become a significant player at the nanoscale and can be potentially used for noncontact transduction of mechanical forces within small devices. In particular, such suggestions have been put forward for both the normal Casimir force [9,10] and the lateral Casimir force, which can be realized in systems with lateral periodic geometrical features such as surface corrugations [11,12] and dielectric heterostructures [13]. Given that the normal force is relatively more difficult to control due to its "catastrophic" nature when it sets in [2], the lateral Casimir force seems to be a more practical option for such device applications.

Recently, this idea has been used to propose a number of simple mechanical devices that could work at the nanoscale and are powered by the lateral Casimir force. These proposed devices include a rack-and-pinion machine with a gap between the rack and the pinion and the rack moving at constant speed in one direction [14] or vibrating laterally [15], an asymmetric ratchet system with a harmonically modulating gap separation [16], and a novel system with two racks and one pinion [17]. While such designs could help with the development of alternative solutions for the tribological problems mentioned above, we are also in need of improving the theoretical methods that are available for the calculation of the Casimir force in systems with complex geometries [18–26].

Here, we investigate the dynamical behavior of a frustrated nanomechanical device made with a pinion sandwiched between two racks that are moving in the same direction and coupled via the lateral Casimir force, as shown schematically in Fig. 1. The device can be controlled using a number of geometrical parameters such as the gap size and is only possible due to the noncontact nature of the interaction between the racks and the pinion. The case of a strongly damped rack-pinion-rack device, so that the inertia can be neglected, is studied in Ref. [17]. The strongly damped system has five distinct behaviors: (i) the pinion could be locked with either rack 1 or rack 2, (ii) the pinion could move along with either rack 1 or rack 2 but with a lower average velocity, and (iii) the pinion could oscillate back and forth without choosing to go with either of the racks. The system can dramatically react to minute changes in the gap size and rack velocities and can thus act as a good sensor. The oscillatory regime could be used to generate a clock signal of tunable frequency. In this paper, we analyze the system in a regime where both dissipation and *inertia* are important. Since the parameter space of the general case is very large, we only focus on the fully symmetric device. We find a variety of different dynamical behaviors including symmetry breaking (so that the pinion will choose to move with one of the racks despite perfect symmetry between the two), fractional average velocity of the pinion, intermittent behavior of the pinion around a neutral average position, and pinion velocities that significantly exceed the rack velocity.

The rest of the paper is organized as follows. Section II reviews the lateral Casimir force, while Sec. III describes the general dynamical formulation of the motion of the pinion. Section IV is devoted to the numerical analysis of the system, which is followed by some discussions and concluding remarks in Sec V.

II. LATERAL CASIMIR FORCE

Consider two plates with harmonic corrugations of identical wavelength λ that are positioned opposite to one an-

*miri@iasbs.ac.ir
†r.golestanian@sheffield.ac.uk

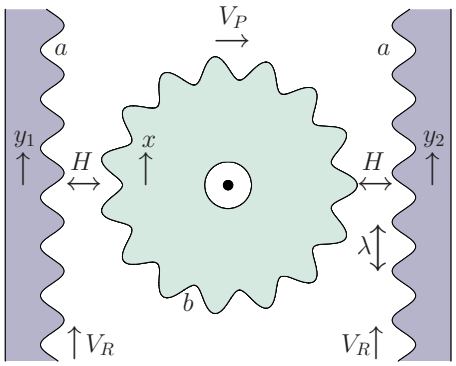

FIG. 1. (Color online) The schematics of the rack-pinion-rack device. The racks and the pinion have sinusoidal corrugations of wavelength λ and amplitudes a and b, respectively. The choice of parallel rack velocities V_R (rather than opposite) frustrates the system, which is only possible because of the noncontact design. The pinion velocity V_P is taken as positive if it is in the direction shown, as a convention.

other with a relative lateral displacement of $x-y$. Due to their interaction with the quantum fluctuations of the electromagnetic vacuum, they experience a lateral Casimir force of the form [11]

$$F_{\text{lateral}} = -F \sin\left[\frac{2\pi}{\lambda}(x-y)\right], \tag{1}$$

where the amplitude F depends on the mean separation of the plates and the amplitude of the corrugations [12,18,19]. The amplitude of the lateral Casimir force for two parallel plates is given as

$$F_{\text{plate}} = \frac{2\pi\hbar c a b A}{\lambda H^5} J(H/\lambda), \tag{2}$$

where a and b are the two amplitudes of the corrugations on the two surfaces, respectively, H is the mean separation between the plates, and A is the surface area of the plates.

In Eq. (2), the "Josephson" coupling function $J(x)$ starts from the constant value of $\pi^2/120$ at small x and decays exponentially at large x [18]. To get a feel for the strength of the lateral Casimir force, one can look at the experimentally measured values for it; for a plate and a sphere of radius 100 μm with $\lambda=1.1$ μm, $H\sim 200-300$ nm, $a=60$ nm, $b=8$ nm, the force is in the 0.1 pN range [12].

III. EQUATION OF MOTION

The system we study consists of two identical corrugated plates (racks) with corrugation amplitude a that sandwich a corrugated cylinder (pinion) with corrugation amplitude b, leaving gaps of size H at either side between the surfaces (see Fig. 1). The pinion experiences a lateral Casimir force from each of the racks; note that the wavelength of the corrugations must be the same on all the three surfaces so that coherent coupling is possible. The amplitude of the lateral Casimir force F, called the *Casimir grip* henceforth, depends on the geometric characteristics of the device and in particular the gap size and the amplitudes of corrugations [12,14,15,18,19].

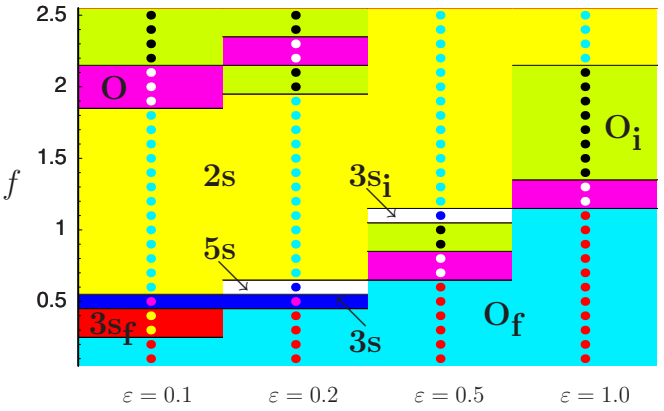

FIG. 2. (Color online) Phase diagram of the dynamical system. The following notation is used in the labels of the different phases. 0 means that the average pinion velocity is zero, while 2s, 3s, and 5s denote the number of possible different states (outcomes) in each region depending on the initial conditions. The subscript "f" denotes no oscillations around the terminal value of (mean) velocity, while the subscript "i" denotes intermittency in the pinion velocity time series, both for the case when the average velocity is zero. The sequence of phases are (0_f, $3s_f$, 3s, 2s, 0, 0_i) for $\varepsilon=0.1$, (0_f, 3s, 5s, 2s, 0_i, 0, 0_i) for $\varepsilon=0.2$, (0_f, 0, 0_i, $3s_i$, 2s) for $\varepsilon=0.5$, and (0_f, 0, 0_i, 2s) for $\varepsilon=1.0$.

The surfaces of the two racks exert opposing lateral Casimir forces on the pinion, which add up to a net torque of $-RF\sin[2\pi(x-y_1)/\lambda]-RF\sin[2\pi(x+y_2)/\lambda]$ that needs to be taken into account in the equation of motion that probes the dynamics of the pinion. This equation is written using the principal coordinate $x=R\theta$, where θ is the angle of rotation and R is the radius of the pinion. Putting in $y_1=y_2=V_Rt$, the equation of motion reads

$$\frac{I}{R}\frac{d^2x}{dt^2}+\frac{\zeta}{R}\frac{dx}{dt} = -RF\sin\left[\frac{2\pi(x-V_Rt)}{\lambda}\right] - RF\sin\left[\frac{2\pi(x+V_Rt)}{\lambda}\right], \tag{3}$$

where I is the moment of inertia of the pinion about its major axis and ζ is the rotational friction coefficient [27]. This dynamical equation needs to be solved with the initial position x_0 and the initial velocity v_0 to determine the possible long-time behaviors of the device.

We can estimate the moment of inertia of the pinion as $I=\frac{1}{2}MR^2=\frac{\pi}{2}\rho LR^4$, assuming it is a uniform cylinder of mass M, density ρ, and height L. This ignores the corrugations, which should be a reasonable approximation for sufficiently large radii. We can also estimate the rotational friction coefficient ζ using a model for the friction involved in the setup. Assuming that the lubrication at the axle (or pivot) on which the pinion is mounted is the main source of friction in the system, we can estimate the friction coefficient as $\zeta \simeq 2\pi\eta Lr^3/h$ for an axle of radius r that is lubricated with a fluid layer of thickness h and viscosity η.

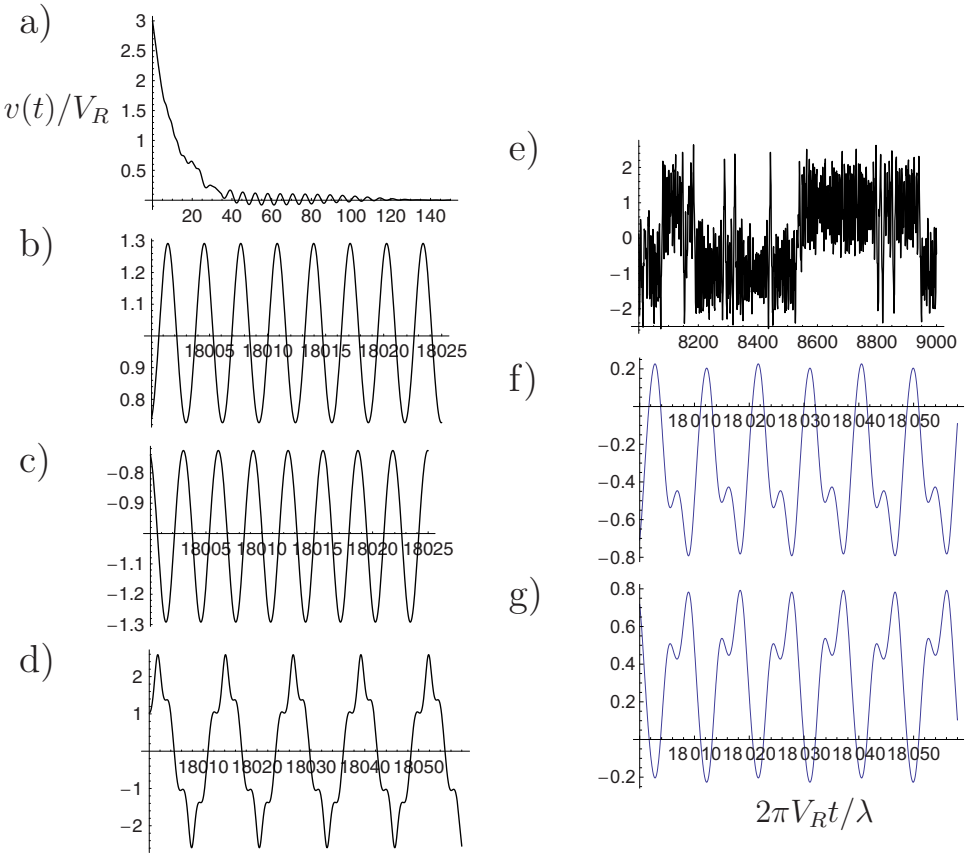

FIG. 3. (Color online) Various types of signals observed for $v(t)$ for different values of f and ε. (a) corresponds to $f=0.1$ and $\varepsilon=0.1$, which belongs to the domain denoted as 0_f in Fig. 2, where the pinion velocity vanishes in the long-time limit. (b) and (c) correspond to $f=1$ and $\varepsilon=0.1$ and represent the cases where the pinion is locked onto one of the racks and the velocity oscillates about $+V_R$ or $-V_R$. (d) corresponds to $f=2$ and $\varepsilon=0.1$, which belongs to the domain denoted as 0 in Fig. 2, and shows a case where the pinion velocity oscillates about zero. (e) corresponds to $f=2$ and $\varepsilon=0.2$, which belongs to the domain denoted as 0_i in Fig. 2, and shows a case where the pinion velocity oscillates in an intermittent manner about zero. (f) and (g) correspond to $f=0.6$ and $\varepsilon=0.2$, which belongs to the domain denoted as 5s in Fig. 2, and represent the cases where the pinion average velocity could be $-0.33V_R$ or $+0.33V_R$, respectively.

In the dynamics of the rack-pinion-rack device, $\lambda/(2\pi)$ and $T=\lambda/(2\pi V_R)$ are the natural units of length and time, respectively. Introducing $\bar{x}=2\pi x/\lambda$ and $\tau=t/T$, the equation of motion can be written as

$$\frac{d^2\bar{x}}{d\tau^2} = -\varepsilon\frac{d\bar{x}}{d\tau} - f\sin\bar{x}\cos\tau, \tag{4}$$

where the dimensionless dissipation coefficient is defined as

$$\varepsilon = \frac{\zeta\lambda}{2\pi I V_R} \tag{5}$$

and the dimensionless Casimir grip is defined as

$$f = \frac{R^2 F\lambda}{\pi I V_R^2}. \tag{6}$$

We also note that Eq. (4) describes a permanent magnet in a periodically oscillating magnetic field [28] or an electron in a standing-wave field [29]. Equation (4) exhibits rich dynamical behaviors such as symmetry-breaking pitchfork bifurcations, period-doubling transitions to chaos, symmetry-restoring attractor-merging crises, and saddle node bifurcations giving rise to new periodic attractors [30].

IV. RESULTS

The nonlinear nature of the dynamics of the system, together with the presence of the inertial term, leads to a rich variety of different behaviors. For example, similar to the device studied in Ref. [15], the system can exhibit *spontaneous symmetry breaking*. The pinion can be locked onto one of the racks, i.e., the average pinion velocity V_P can be either $+V_R$ or $-V_R$. According to Chirikov [31], the above system at $\varepsilon=0$ exhibits chaotic motion for $f>\frac{1}{2}$. The addition of the friction term to the dynamical equation will make analytical study of the dynamical system more cumbersome.

Here, instead of embarking on a full study of this system, we focus on the average pinion velocity in the long-time limit and try to identify the different dynamical regimes that can exist depending on the initial conditions and the value of the two parameters ε and f. We have numerically studied Eq. (4) for $\varepsilon\in[0.1,0.2,0.5,1]$ and $f\in[0.1,0.2,0.3,\ldots,2]$. In this range of parameters, the inertia term plays a key role and is a distinctly different regime as compared to the dissipative

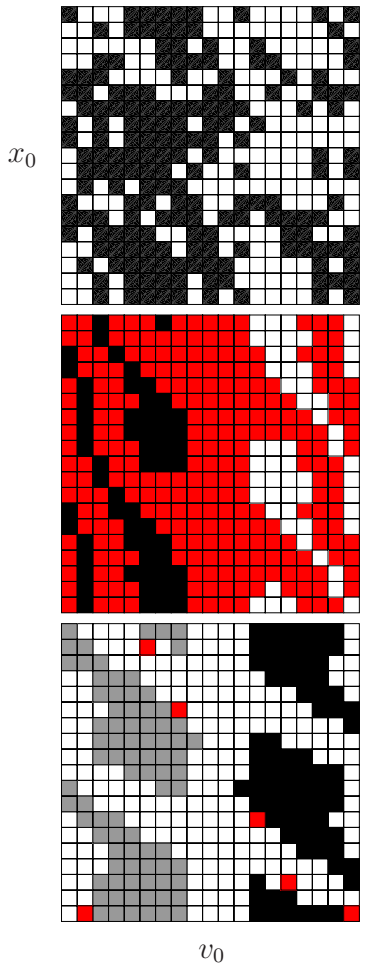

FIG. 4. (Color online) In many of the regions in the phase diagram of Fig. 2, different initial conditions lead to different average velocities. x_0 is between $-\lambda$ and λ (20 points) and v_0 is between $-3V_R$ and $3V_R$ (20 points). Top: $f=1.5$ and $\varepsilon=0.1$ (2s), white means $V_P=V_R$, and black means $V_P=-V_R$. Middle: $f=0.3$ and $\varepsilon=0.1$ ($3s_f$), red means $V_P=0$, white means $V_P=V_R$, and black means $V_P=-V_R$. Bottom: $f=0.6$ and $\varepsilon=0.2$ (5s), white means $V_P=0$, black means $V_P=V_R$, gray means $V_P=-V_R$, and red means $V_P=0.33V_R$ if $v_0>0$ and $V_P=-0.33V_R$ if $v_0<0$.

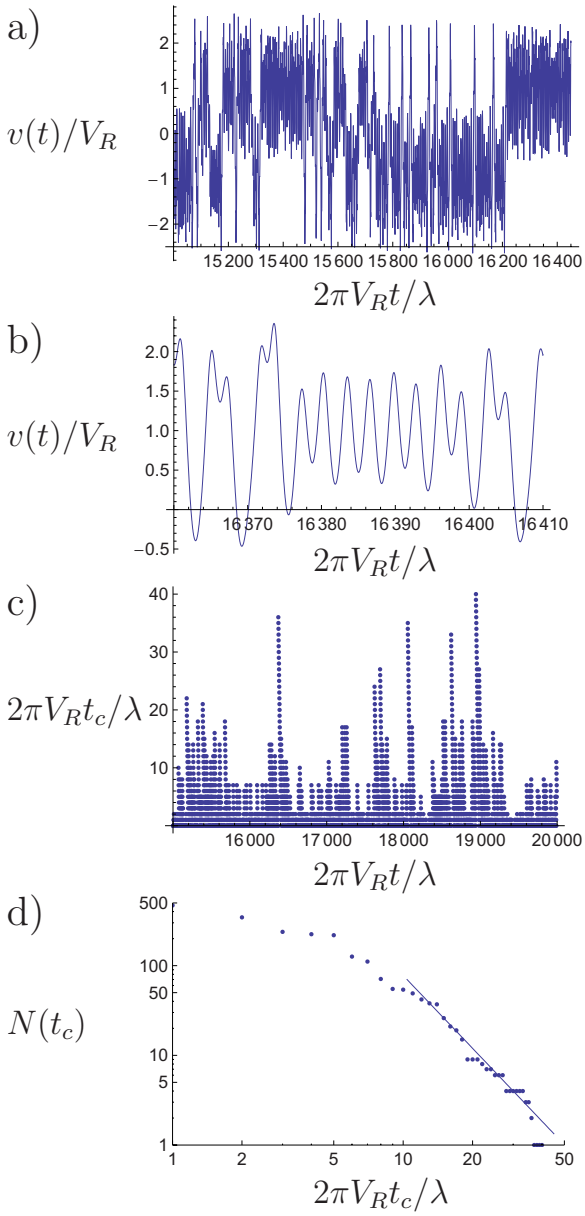

FIG. 5. (Color online) (a) The intermittent velocity signal for $f=2$ and $\varepsilon=0.2$ (within the 0_i phase) corresponding to $x_0=3\lambda/(2\pi)$ and $v_0=3V_R$. (b) shows a portion of the time series, indicating large correlation times. In (c), the correlation time t_c is calculated for the section of the time series between $0.75\times 20\,000$ and 20 000 time steps. In (d), the histogram of correlation times $N(t_c)$ is plotted vs the correlation time in a log-log scale. The line that goes through the data has a slope of -2.7 and is a guide to the eyes.

limit of the same system studied in Ref. [17]. In our numerical investigations of the behavior of the dynamical system, we limit ourselves to the initial conditions $\bar{x}_0 \in [-2\pi, -34\pi/19, \ldots, 34\pi/19, 2\pi]$ and $\bar{x}_0' \in [-3, -51/19, \ldots, 51/19, 3]$. Of course, one may identify other dynamical regimes choosing parameters ε, f, $\bar{x}_0$, and $\bar{x}_0'$ not listed here.

The system exhibits a variety of different behaviors that we probe by calculating the pinion velocity $v(t)$ at long times and its average value V_P. Figure 2 delineates the different possible types of behavior in the space of the parameters ε and f and Fig. 3 shows a number of sample time series for the pinion velocity corresponding to these different phases. For small values of f, the system is driven to a fixed point at $\bar{x}(\tau)=n\pi$ (depending on the initial conditions), where n is an integer. In this phase, which is denoted as 0_f in Fig. 2, the average pinion velocity is zero as can be seen in Fig. 3(a). In the regions denoted as 0 in Fig. 2, the pinion velocity oscillates about a vanishing average. In the region labeled as 2s in Fig. 2, the average pinion velocity V_P could be either $-V_R$ or $+V_R$, depending on the initial conditions. Figures 3(b) and 3(c) show sample pinion velocity signals oscillating about $-V_R$ or $+V_R$, while Fig. 4 shows the different regions in the space of initial conditions that could lead to different final behaviors. While in phase 0, the pinion velocity oscillates regularly around a zero average, although instantaneous velocities could be even more than a factor of 2 larger than the rack velocity as Fig. 3(d) shows, in another region denoted

as 0_i in Fig. 2 the system could exhibit a net vanishing velocity with an intermittent signal that oscillates randomly between values near $-V_R$ and $+V_R$, as shown in Fig. 3(e).

In a number of regions in Fig. 2, the system evolves to an average pinion velocity of $-V_R$, 0, or $+V_R$ depending on initial conditions (see Fig. 4). When the average velocity in these regions is $-V_R$ or $+V_R$, the time series oscillates about the average value as shown in the example of Figs. 3(b) and 3(c). When, however, the average velocity is zero in these regions, the system could exhibit the three behaviors described above. These regions are denoted as $3s_f$ when the average velocity decays to zero with no oscillations, 3s when the average velocity oscillates regularly about zero, and $3s_i$ when it oscillates intermittently about zero. Finally, a small region in Fig. 2, denoted as 5s, was found where the system can evolve to five different states with final average pinion velocities of $-V_R$, $-0.33V_R$, 0, $+0.33V_R$, and $+V_R$ depending on the initial conditions, as can be seen in Fig. 4. Figures 3(f) and 3(g) show typical velocity time series whose averages are $-0.33V_R$ and $+0.33V_R$, respectively.

V. DISCUSSION

The combination of inertia and the nonlinear frustrated coupling in the dynamical system could lead to a wide range of behaviors, as summarized in the phase diagram of Fig. 2. There are several remarkable features in the results presented in Sec. IV. At small values of f, the system is in the phase 0_f for all values of ε. Increasing the value of f then drives the system into several other phases depending on the value of ε. These transitions do not always follow our intuitions. For example, upon increasing f, the system goes into the phases where several states could coexist, which could be interpreted as being cause by the stronger Casimir grip. However, further increasing f could drive the system out of these phases into the symmetric phase that oscillates between the two states. In other words, increasing the strength of the bond between the racks and the pinion first leads to symmetry breaking and then into a re-entrant oscillatory double-bond between the pinion and both racks. This can be achieved by decreasing the gap size H or the rack velocity V_R to increase the coupling strength f [see Eq. (6)]. Another interesting feature is that unlike the fully dissipative case where the pinion velocity could at most reach the velocity of one of the racks, the inertia in the system can cause the value of the velocity to overshoot significantly, as can be seen in the example of Fig. 3(d). The existence of the fractional velocity of $\pm 0.33V_R$ is also very interesting in the sense that in the system effectively oscillates between the two states of but with unequal weight for each.

Another interesting feature of the dynamical behaviors of the system is the presence of intermittency in the velocity time series. Figure 5(a) shows a pinion velocity signal that consists of batches that oscillate about $+V_R$ alternating with batches that oscillate about $-V_R$, with an overall average of zero. A zoom into a portion of the signal at long times, shown in Fig. 5(b), demonstrates long correlation times. To probe this behavior in a quantitative way, we have defined a correlation time t_c and measured its statistical properties. The correlation time is defined as follows. We first quantize the velocity signal by setting it to +1 if it is positive and to −1 if it is negative (in units of V_R). Then at each time t, we probe the signal and extract the time that it takes until the digitized velocity signal switches over from +1 to −1; we call this time $t_c(t)$. Figure 5(c) shows the values of these correlation times as a function of time in an intermittent solution of the dynamical system. We then use this time series to extract the distribution function of the correlation times $N(t_c)$, which is defined as the number of occurrences of a certain value of t_c in a given portion of the time series. This distribution is plotted in Fig. 5(d) in a log-log scale and as can be seen, it shows that a full spectrum of correlation times is present in the dynamics. Moreover, our numerical results suggest that the long-time tail of the distribution might have an algebraic decay with an exponent −2.7, although our limited numerical studies are not sufficient to verify this behavior in a satisfactory way.

In its strongly damped regime, the fully symmetric rack-pinion-rack device could be used to generate a clock signal of tunable frequency [17]. We find that the weakly damped pinion may choose to move with one of the racks. In practice, the pinion is mounted on an axle and the main source of friction in the system comes from the lubrication at the axle. Our analysis shows that one does not face the reduction of friction as a major obstacle to realize the mechanical clock.

In conclusion, we have studied the dynamical behavior of a frustrated mechanical device that can be made at small scale using the lateral Casimir force as the main force transduction mechanism. The combination of inertia, friction, frustration, and nonlinearity of the dynamical coupling has led to a rich phase diagram of deterministic and chaotic regimes. This study could help us toward understanding the potential benefits of such nanomechanical devices in future directions of mechanical engineering.

ACKNOWLEDGMENTS

R.G. wishes to thank the ESF Research Network CASIMIR for providing excellent opportunities for discussion on the Casimir effect and related topics. This work was supported by EPSRC under Grant No. EP/F036167/1.

[1] M. P. de Boer and T. M. Mayer, MRS Bull. **26**, 302 (2001).
[2] E. Buks and M. L. Roukes, Phys. Rev. B **63**, 033402 (2001).
[3] A. Socoliuc, E. Gnecco, S. Maier, O. Pfeiffer, A. Baratoff, R. Bennewitz, and E. Meyer, Science **313**, 207 (2006).
[4] J. Y. Park, D. F. Ogletree, P. A. Thiel, and M. Salmeron, Science **313**, 186 (2006).
[5] R. W. Carpick, Science **313**, 184 (2006).
[6] H. B. G. Casimir, Proc. K. Ned. Akad. Wet. **51**, 793 (1948).

[7] M. Bordag, U. Mohideen, and V. M. Mostepanenko, Phys. Rep. **353**, 1 (2001).
[8] M. Bordag, G. L. Klimchitskaya, U. Mohideen, and V. M. Mostepanenko, *Advances in the Casimir Effect* (Oxford University Press, Oxford, 2009).
[9] H. B. Chan, V. A. Aksyuk, R. N. Kleiman, D. J. Bishop, and F. Capasso, Science **291**, 1941 (2001).
[10] H. B. Chan, V. A. Aksyuk, R. N. Kleiman, D. J. Bishop, and F. Capasso, Phys. Rev. Lett. **87**, 211801 (2001).
[11] R. Golestanian and M. Kardar, Phys. Rev. Lett. **78**, 3421 (1997).
[12] F. Chen, U. Mohideen, G. L. Klimchitskaya, and V. M. Mostepanenko, Phys. Rev. Lett. **88**, 101801 (2002); Phys. Rev. A **66**, 032113 (2002).
[13] A. Azari, H. S. Samanta, and R. Golestanian, New J. Phys. **11**, 093023 (2009).
[14] A. Ashourvan, M. F. Miri, and R. Golestanian, Phys. Rev. Lett. **98**, 140801 (2007).
[15] A. Ashourvan, M. F. Miri, and R. Golestanian, Phys. Rev. E **75**, 040103(R) (2007).
[16] T. Emig, Phys. Rev. Lett. **98**, 160801 (2007).
[17] M. F. Miri and R. Golestanian, Appl. Phys. Lett. **92**, 113103 (2008).
[18] T. Emig, A. Hanke, R. Golestanian, and M. Kardar, Phys. Rev. A **67**, 022114 (2003).
[19] R. B. Rodrigues, Paulo A. Maia Neto, A. Lambrecht, and S. Reynaud, Phys. Rev. Lett. **96**, 100402 (2006).
[20] T. Emig, Europhys. Lett. **62**, 466 (2003); R. Büscher and T. Emig, Phys. Rev. Lett. **94**, 133901 (2005).
[21] R. Golestanian, Phys. Rev. Lett. **95**, 230601 (2005); Phys. Rev. A **80**, 012519 (2009).
[22] A. Lambrecht and V. N. Marachevsky, Phys. Rev. Lett. **101**, 160403 (2008).
[23] A. Rodriguez, M. Ibanescu, D. Iannuzzi, F. Capasso, J. D. Joannopoulos, and S. G. Johnson, Phys. Rev. Lett. **99**, 080401 (2007); A. Rodriguez, M. Ibanescu, D. Iannuzzi, J. D. Joannopoulos, and S. G. Johnson, Phys. Rev. A **76**, 032106 (2007); A. W. Rodriguez, J. D. Joannopoulos, and S. G. Johnson, *ibid.* **77**, 062107 (2008).
[24] S. Pasquali and A. C. Maggs, J. Chem. Phys. **129**, 014703 (2008); Phys. Rev. A **79**, 020102(R) (2009).
[25] F. C. Lombardo, F. D. Mazzitelli, and P. I. Villar, J. Phys. A **41**, 164009 (2008).
[26] I. Cavero-Peláez, K. A. Milton, P. Parashar, and K. V. Shajesh, Phys. Rev. D **78**, 065018 (2008); **78**, 065019 (2008).
[27] In Eq. (3), a constant offset in the argument of the sine functions due to the positioning of the pinion can be eliminated by a suitable choice of the origin for x and t.
[28] H. Meissner and G. Schmidt, Am. J. Phys. **54**, 800 (1986); K. Briggs, *ibid.* **55**, 1083 (1987); F. C. Moon, J. Cusumano, and P. J. Holmes, Physica D **24**, 383 (1987).
[29] D. F. Escande and F. Doveil, Phys. Lett. A **83**, 307 (1981); J. Stat. Phys. **26**, 257 (1981); D. F. Escande, Phys. Rep. **121**, 165 (1985).
[30] S.-Y. Kim, J. Phys. A **32**, 6727 (1999).
[31] B. V. Chirikov, Phys. Rep. **52**, 263 (1979).